# Weak value amplification for nonunitary evolution

Wei-Tao Liu,[1,2,*] Julián Martínez-Rincón,[3] and John C. Howell[4,5]

[1]*College of Liberal Arts and Sciences, National University of Defense Technology, Changsha 410073, China*

[2]*Interdisciplinary Center of Quantum Information, National University of Defense Technology, Changsha 410073, China*

[3]*Department of Physics, Stanford University, Stanford, California 94305, USA*

[4]*Department of Physics and Astronomy and Center for Coherence and Quantum Optics, University of Rochester, Rochester, New York 14627, USA*

[5]*Racah Institute of Physics, The Hebrew University of Jerusalem, 91904 Jerusalem, Israel*

(Received 3 May 2019; published 23 July 2019)

We discuss interferometric parameter estimation of the amplitude, instead of the phase, via weak value amplification. The considered weak interaction introduces modulation on the amplitude of the wave function; therefore, the two-party state experiences a nonunitary evolution. With the same pre- and postselection states as those of original weak value amplification, a much larger anomalous amplification factor can be attained. The shift in the intensity profile at the dark port and the signal-to-noise ratio for the parameter of interest get further amplified by the weak value, compared to phase-based weak value amplification. Although the nonunitary evolution introduces loss, more information about the parameter of interest can be extracted. Thus the weak value amplification is extended to measurement of amplitude and nonunitary processes. We also discuss possible applications of this idea for precisely measuring tiny rotations or enhancing the image contrast of transparent objects.

DOI: 10.1103/PhysRevA.100.012125

## I. INTRODUCTION

Introduced by Aharonov *et al.* [1], the weak value amplification effect is nowadays employed as a metrological technique to precisely measure small parameters, which can convert a small change in a system-meter coupling parameter into a large change in a meter variable. The system is prepared in a specified state (preselection state), then gets coupled to the meter via a weak interaction and projected to a postselection state. To obtain such an amplification, the pre- and postselection states are set to be nearly orthogonal; thus, only a small postselected fraction of the events experiencing the amplified meter variable are measured, and nearly all the Fisher information about the parameter of interest can be retrieved. In this point of view, this effect helps to concentrate the Fisher information about the measured parameter into a small number of collected events [2–4]. For the ideal case, the signal-to-noise ratio (SNR) of the measured parameter turns out to be the same as if the measurements were made directly and collecting all the events [5].

Experimentally, ultrasensitive measurements have been achieved based on weak value amplification for optical-beam deflections [6–12], phase shifts [13–15], frequency shifts [5], velocities [16], temporal shifts [17,18], angular shifts [19,20], and even temperature changes [21]. Weak value amplification for gravitational sensing is also discussed [22]. Considering technical noise, researchers are trying to clarify advantages and disadvantages of the weak value amplification technique [2,3,17,23–26] compared to standard methods. At the same time, increasing the efficiency of the weak value amplification technique with the help of entanglement [4] or power recycling is also discussed [27,28].

Many weak value measurement experiments have been demonstrated using interferometers [29,30]. The system is set to be a qubit, using eigenstates of a binary operator $\hat{A}$, such as two paths in an interferometer or two orthogonal polarization states of photons, while the meter is prepared in a continuous state with the amplitude profile usually set to be Gaussian with respect to a continuous variable $q$. The weak interaction couples the system and the meter, which can be described as a unitary evolution $\hat{U} = \exp(-ig\hat{q} \times \hat{A})$, and eventually causes a small phase shift between two eigenstates of the system. For interferometric weak values, the meter state is measured in the "dark" port of the interferometer, which is actually the destructive interference output. The shift in the meter is inversely proportional to the relative phase of the arms of the interferometer. Taking advantage of this anomalous amplification, the parameter of interest $g$ can be precisely retrieved. Since it is actually measuring the phase shift between two paths, let us denote it as the phase-modulation weak value amplification (PWVA). In this paper, we extend weak value amplification into the amplitude regime. In such amplitude-modulation weak value amplification (AWVA), the whole system experiences a nonunitary process since the weak interaction introduces changes in the amplitude or intensity of the wave function instead of the phase. Compared to PWVA, the shift of the meter state and the SNR are magnified by a factor of the same order as the weak value.

## II. THEORY

First, let us briefly review the idea of PWVA, taking imaginary weak value amplification as an example. As shown

*wtliu@nudt.edu.cn

 

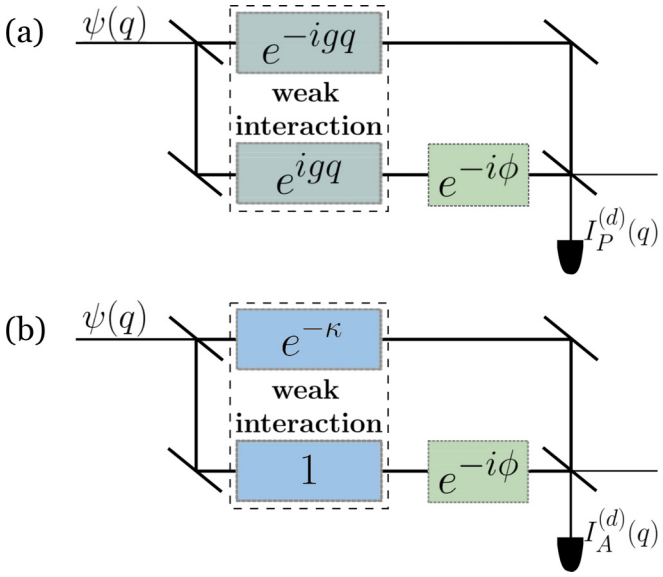


FIG. 1. Schematic diagram of interferometric weak-value amplification. Two degrees of freedom of photons are usually employed, one of which can be treated as a qubit and serves as the system, while the other one is in a continuous variable state and serves as the meter. The system and the meter get slightly entangled by the weak interaction. (a) For phase-modulation weak value amplification, the two-party state experiences a unitary evolution during weak interaction, and a relative phase between two eigenstates of the qubit system is introduced. (b) For amplitude-modulation weak value amplification, the two-party state experiences a nonunitary evolution during weak interaction, and modification in amplitude of one of two qubit states is introduced. By controlling the postselection phase $\phi$, only a small number of events will be detected at the dark port, and an anomalous amplification will be obtained in the meter state.

in Fig. 1(a), the initial state is prepared as $\psi(q) \times |\Psi_i\rangle$, where $\psi(q) = \frac{1}{N} \exp(-\frac{(q-q_0)^2}{4\sigma^2})$ defines the Gaussian profile of the meter state and $|\Psi_i\rangle = (|0\rangle + |1\rangle)/\sqrt{2}$ is the preselection state of the system. Here $\sigma^2$ is the variance of the profile, and $\{|0\rangle, |1\rangle\}$ are eigenstates of the qubit system, corresponding to two paths in the interferometer. Then the system gets coupled to the meter by the weak interaction. The unitary evolution is written in the qubit basis as

$$U_P = \begin{pmatrix} e^{-igq} & 0 \\ 0 & e^{igq} \end{pmatrix}, \tag{1}$$

where $\hat{A}$ is defined as the which-path operator $\hat{A} = |0\rangle\langle 0| - |1\rangle\langle 1|$. By measuring the qubit system in a postselection state of $|\Psi_f\rangle = (|0\rangle - e^{-i\phi}|1\rangle)/\sqrt{2}$, the output at the dark port turns out to be

$$\begin{aligned} I_P^{(d)}(g,q) &\propto |\langle\Psi_f|U_P|\Psi_i\rangle\psi(q)|^2 \\ &\propto \sin^2\left(\frac{\phi}{2} - gq\right) \exp\left(-\frac{(q-q_0)^2}{2\sigma^2}\right). \end{aligned} \tag{2}$$

Under the weak value approximation, i.e., $g\sigma \cot(\frac{\phi}{2}) \ll 1$,

$$I_P^{(d)}(g,q) \propto \sin^2\left(\frac{\phi}{2}\right) \exp\left(-\frac{\left[q - q_0 + 2g\sigma^2 \cot\left(\frac{\phi}{2}\right)\right]^2}{2\sigma^2}\right). \tag{3}$$

Compared to the initial intensity profile, the profile of the output gains a shift of $2g\sigma^2 \cot(\frac{\phi}{2})$; therefore, the parameter of interest $g$ can be retrieved by estimating $\langle q\rangle$ [31]. The amount of Fisher information about $g$ is given by

$$\mathcal{I}_P = 4N\sigma^2 \cos^2\left(\frac{\phi}{2}\right), \tag{4}$$

where $N$ is the total number of input photons, with the number of detected photons being $N \sin^2(\frac{\phi}{2})$, assuming the whole setup is lossless. In the ideal case, shot noise is the only source of error; thus, the minimal uncertainty of $g$ can be well estimated by the Cramér-Rao bound as

$$\Delta g_P^{\mathrm{CRB}} = 1/\sqrt{\mathcal{I}_P} = \frac{1}{2\sqrt{N}\sigma \cos\left(\frac{\phi}{2}\right)}. \tag{5}$$

Accordingly, the best SNR is

$$R_P = 2g\sqrt{N}\sigma \cos\left(\frac{\phi}{2}\right). \tag{6}$$

From Eq. (1), the whole state after the weak interaction can be written as

$$\frac{1}{\sqrt{2}}[|0\rangle \times e^{-igq}\psi(q) + |1\rangle \times e^{igq}\psi(q)]. \tag{7}$$

This means that when considering changes in the state of the meter, the weak interaction shifts the phase of the state according to the value of the qubit as well as the parameter $g$. The phases of states on both paths are shifted by the same distance, in opposite directions. On the contrary, we consider the case of shifting the conjugate variable of the phase, that is, doing the weak interaction in such a way that the amplitude of the eigenstate will be modified according to the value of the qubit and the parameter of interest. Assume the weak interaction introduces different small absorptions (or losses) according to different eigenstates of the qubit system. Therefore, the whole two-party system will experience a nonunitary evolution caused by a weak interaction. With the weak interaction approximation, anomalous amplification can also be attained in this situation, which even gains additional magnification compared to PWVA. Let us denote it as amplitude-modulation weak value amplification. The operation matrix represented in the qubit basis can be written as

$$O_A = \begin{pmatrix} e^{-\kappa} & 0 \\ 0 & 1 \end{pmatrix}, \tag{8}$$

where $\kappa \ll 1$ is related to loss on the path and it can be a real-valued function of $g$ and $q$. Employing the same preselection and postselection states as in PWVA, the output at the dark port reads

$$\begin{aligned} I_A^{(d)}(\kappa,q) &\propto |\langle\Psi_f|O_A|\Psi_i\rangle\psi(q)|^2 \\ &= \frac{1}{4}|e^{-\frac{\kappa}{2}}(e^{-\frac{\kappa}{2}}e^{-i\frac{\phi}{2}} - e^{\frac{\kappa}{2}}e^{i\frac{\phi}{2}})\psi(q)|^2 \\ &= \frac{1}{4}e^{-\kappa}(e^{\frac{\kappa}{2}} + e^{\frac{-\kappa}{2}})^2 \sin^2\left(\frac{\phi}{2}\right) \end{aligned}$$

$$\times\left[\frac{(e^{\frac{-\kappa}{2}}-e^{\frac{\kappa}{2}})^2}{(e^{\frac{-\kappa}{2}}+e^{\frac{\kappa}{2}})^2}\cot^2\left(\frac{\phi}{2}\right)+1\right]|\psi(q)|^2$$

$$\approx \sin^2\left(\frac{\phi}{2}\right)\left[1+\frac{\kappa^2}{4}\cot^2\left(\frac{\phi}{2}\right)\right]\exp\left(-\frac{(q-q_0)^2}{2\sigma^2}\right). \quad (9)$$

Setting $\kappa=\sqrt{4gq}$ and considering the weak interaction approximation, i.e., $g\sigma\cot^2(\frac{\phi}{2})\ll 1$ (see the Appendix for details), we can obtain

$$I_A^{(d)}(g,q)\propto \sin^2\left(\frac{\phi}{2}\right)\exp\left(-\frac{\left[q-q_0-g\sigma^2\cot^2\left(\frac{\phi}{2}\right)\right]^2}{2\sigma^2}\right). \quad (10)$$

With respect to the initial intensity profile of the input state, the output gains a shift with the amount of $g\sigma^2\cot^2(\frac{\phi}{2})$. As is the case in PWVA, the expectation value of $q$, $\langle q\rangle$, is the optimal estimator for $g$. By measuring the intensity profile at the dark port and comparing it with the initial intensity profile, the parameter of interest $g$ can be retrieved, with Fisher information of (details of the derivation are shown in the Appendix)

$$\mathcal{I}_A = N\sigma^2\cos^2\left(\frac{\phi}{2}\right)\cot^2\left(\frac{\phi}{2}\right)$$

$$= \frac{1}{4}\cot^2\left(\frac{\phi}{2}\right)\mathcal{I}_P. \quad (11)$$

Here $N$ is also the number of input photons, with the number of detected photons being $\sim N\sin^2(\frac{\phi}{2})$. Therefore, the minimal uncertainty or Cramér-Rao bound of estimated $g$ will be

$$\Delta g_A^{\mathrm{CRB}} = \frac{1}{\sqrt{N}\sigma\cos\left(\frac{\phi}{2}\right)\cot\left(\frac{\phi}{2}\right)} = \frac{\Delta g_P^{\mathrm{CRB}}}{\frac{1}{2}\cot\left(\frac{\phi}{2}\right)}. \quad (12)$$

Then the best SNR we can get turns out to be

$$R_A = g\sqrt{N}\sigma\cos\left(\frac{\phi}{2}\right)\cot\left(\frac{\phi}{2}\right) = \frac{1}{2}\cot\left(\frac{\phi}{2}\right)R_P. \quad (13)$$

Let us do a further comparison between AWVA and PWVA. Under the same pre- and postselections, we obtain additional anomalous amplification in the shift of the output intensity profile for AWVA by a factor of $\frac{1}{2}\cot(\frac{\phi}{2})$ compared to PWVA. The factor is exactly half the imaginary part (also the absolute value in this case) of the weak value of the which-path operator $\hat{A}$, given by $A_W=\langle\Psi_f|\hat{A}|\Psi_i\rangle/\langle\Psi_f|\Psi_i\rangle=-i\cot(\frac{\phi}{2})$. Such an amplification provides the possibility of recovering more Fisher information about the parameter of interest by a factor of $\frac{1}{4}\cot^2(\frac{\phi}{2})$. Although the weak interaction introduces loss, more information about $g$ can be extracted. Therefore, AWVA is more efficient than PWVA since more information can be obtained with the same number of input photons. The idea of power recycling [27,28] can also be employed into our protocol, which will further improve the performance. At the same time, the smallest uncertainty of estimated $g$ is smaller, which implies that AWVA promises higher precision and higher sensitivity. By comparing Eqs. (13) and (6), the signal-to-noise ratio of AWVA is also magnified by a factor proportional to the weak value with respect to that of PWVA.

In fact, all the differences between amplitude-modulation and phase-modulation weak value amplifications arise from the weak interaction since we consider a similar setup and the same pre- and postselection states. First, we introduce shifts in the amplitude of the eigenstates, instead of the phase. Thus, the two-party state experiences a nonunitary evolution at the weak interaction procedure, different from that of PWVA. So we are extending the idea of weak value amplification to nonunitary processes. Second, the shifts in amplitude vary in a nonlinear way with respect to the meter variable and parameter of interest, while the shift in phase for PWVA is a linear function. This is one of the reasons for getting the additional factor of $\frac{1}{2}\cot(\frac{\phi}{2})$ in the shift. Notice that the shift is introduced only in the intensity profile at the dark port, instead of wave function itself, as is the case in PWVA (not shown in the above formulas).

## III. DISCUSSION ON POSSIBLE APPLICATIONS

We now discuss possible applications of our proposed larger anomalous amplification. Suppose we are interested in precisely measuring a tiny rotation speed $\omega$, that is, setting $g=\omega$. We can choose the meter variable $q$ to be time $t$. Therefore, the initial state will be prepared in the Gaussian pulse with an intensity profile of $I(t)=I_0\exp[-(t-t_0)^2/(2\tau^2)]$, where $\tau$ parametrizes the length of the pulse. The pre- and postselections can be performed using a Sagnac interferometer, with the clockwise and counterclockwise beams spatially separated, as shown in Fig. 2. The input laser beam is separated and recombined on the polarization-independent 50:50 beam splitter. The relative phase, which can be controlled, determines the postselected output state of the interferometer. To perform the weak interaction required in our protocol, a nonlinear attenuation wheel can be inserted in one path. To get the nonlinear behavior, the distribution of the transmission coefficient of the wheel ($W_1$ in Fig. 2) can be customized as $e^{-\sqrt{4\theta}}$, where $\theta$ is the angular position on the plane of the wheel. When the wheel is rotating at an unknown speed of $\omega$ such that $\theta=\omega t$, the weak interaction will introduce the required amplitude modulation. With the output at the dark port recorded and compared to the initial intensity profile, the time shift of the profile can be estimated, which is expected to be $\omega\tau^2\cot^2(\frac{\phi}{2})$; thus, $\omega$ can be retrieved.

For comparison, the same setup can be employed to measure such a rotation using the PWVA technique, except for the weak interaction part. As was shown in [32], a combination of quarter- and half-quarter-wave plates can help transfer the rotation into phase modulation, taking the place of $W_1$ and $W_2$ in Fig. 2. It is no longer necessary for two beams to be spatially separated. Setting the fast axis of the quarter-wave plates at specific angles according to the polarization state of the input laser, phase shifts in both beams in the amount of $2\omega t$ will be introduced when rotating the half-wave plate at a speed of $\omega$. Since two beams head through the wave-plate combination from opposite directions, the phases of the two beams will be shifted in opposite directions, as required. With the same Gaussian pulse and postselection phase, the output intensity profile at the dark port will be shifted by $4\omega\tau^2\cot(\frac{\phi}{2})$ with respect to the input intensity profile. Therefore, AWVA

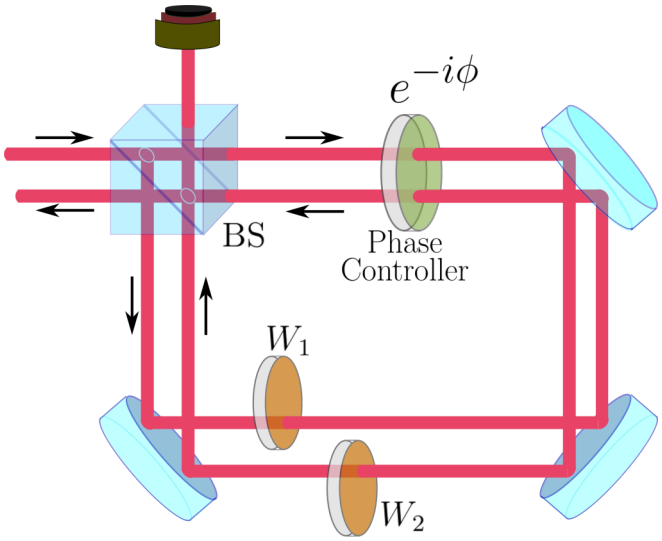


FIG. 2. Schematic diagram for application of amplitude-based weak value amplification. The setup consists of a Sagnac interferometer, with two beams spatially separated. BS is a polarization-independent 50:50 beam splitter, and the phase controller provides the postselection phase by controlling the relative phase between two paths. The plate $W_2$ is a uniformly distributed plate to balance the optical length in two beams. For precision measurement of rotation velocity, $W_1$ is a customized attenuation wheel with the transmission coefficient being $e^{-\sqrt{4\theta}}$, which is rotating at an angular velocity of $\omega$. For the imaging case, $W_1$ is the object of interest, which is a low-contrast transparent object. An additional optical imaging system might be required, which is not considered here.

gains larger amplification by a factor of $\frac{1}{4}\cot(\frac{\phi}{2})$ compared to PWVA.

Another possible application of AWVA is to enhance the image contrast for transparent objects. The setup shown in Fig. 2 can also be used for such imaging. Suppose the area illuminated by the beam on $W_1$ is the object of interest and the transmission ratio contains a certain spatial distribution $T(x) = |e^{-\kappa(x)}|^2$, where $x$ is the transverse position on $W1$. To obtain an image is to retrieve the distribution of $T$ or $\kappa$. Assuming the values of $\kappa$ are small over the whole object, the image of such an object will have low contrast if imaged directly by illuminating and detecting with a regular optical imaging system and array detectors. From Eq. (9), the output at the dark port will also display the spatial distribution, which is related to the distribution of $\kappa$. This will provide information for reconstructing an image of the object with higher contrast due to the anomalous amplification effect. To balance the optical length between two paths, a uniformly distributed plate $W_2$ is employed. The spatial distribution of $\kappa$ will be reflected in the spatial intensity distribution at the dark port, with an amplification factor. The amplification factor can be controlled by the postselection phase $\phi$. An additional optical imaging system might be required to reconstruct the image.

Although we presented our protocol in a way similar to the imaginary weak value, the idea of modulation in amplitude can be extended to other weak-value-based techniques. The key point is to design proper weak interaction to gain the magnification factor. It is worth exploring other possible applications.

## IV. CONCLUSION

In conclusion, we extended the idea of weak value amplification to a nonunitary process and proposed an amplitude-modulation weak value amplification technique, which is more efficient and sensitive than the original weak value amplification. By modulating the states in amplitude instead of phase, the weak interaction between the system and meter introduces a nonunitary evolution for the two-party state. Compared to the phase-based weak value technique, the shift in the meter state can be greatly amplified due to the opportunity of introducing amplitude modulation nonlinearly depending on the parameter of interest. The precision of estimation and signal-to-noise ratio are all improved by a factor of $\frac{1}{2}\cot(\frac{\phi}{2})$. We also discussed possible applications of our proposed protocol for precisely estimating rotation speed and high-contrast imaging.

## ACKNOWLEDGMENTS

W.-T.L. is supported by the National Natural Science Foundation of China under Grant No. 11774431 and the Science and Technology Project of Hunan Province (2017RS3043).

## APPENDIX: DETAILS OF DERIVATION

For both cases, with the input meter state $\psi(q) = \frac{1}{\mathcal{N}}\exp(-\frac{(q-q_0)^2}{4\sigma^2})$, the intensity distribution of the input can be written as $I_{in} = N\frac{1}{\mathcal{N}_m}\exp(-\frac{(q-q_0)^2}{2\sigma^2})$, with $N$ being the total number of input photons and $\mathcal{N}_m$ being the normalization factor for the probability distribution.

Fisher information quantitatively measures the maximum amount of information that can be extracted about an unknown parameter ($g$ in our case) from a random variable $q$. It can be calculated as the variance of the score, which is a measure of the sensitivity of the probability distribution at the detected port with respect to the parameter $g$. The probability distribution at the dark port for AWVA is $f_A = \frac{1}{\mathcal{N}^2}\exp(-\frac{[q-q_0-g\sigma^2\cot^2(\frac{\phi}{2})]^2}{2\sigma^2})$, while for PWVA the probability distribution is $f_P = \frac{1}{\mathcal{N}^2}\exp(-\frac{(q-q_0+2g\sigma^2\cot(\frac{\phi}{2}))^2}{2\sigma^2})$. For both cases, the number of detected photons is $N\sin^2(\frac{\phi}{2})$. From the probability distributions, the score is defined as

$$V(g,q) = \frac{\partial}{\partial g}\ln f_k(g,q). \tag{A1}$$

Here $k = P, A$ refers to the cases of PWVA and AWVA, respectively. In both cases, the mean value of the score vanishes,

$$\begin{aligned}\langle V\rangle &= \int f_k\left[\frac{\partial}{\partial g}\ln f_k(g,q)\right]dq \\ &= \frac{\partial}{\partial g}\left[\int f_k(g,q)dq\right] \\ &= 0.\end{aligned} \tag{A2}$$

Thus, the expression of the Fisher information of $g$ appears,

$$\begin{aligned}\mathcal{I}_k &= N\sin^2\left(\frac{\phi}{2}\right)\langle V^2\rangle \\ &= N\sin^2\left(\frac{\phi}{2}\right)\left\langle\left[\frac{\partial}{\partial g}\ln f_k\right]^2\right\rangle \\ &= N\sin^2\left(\frac{\phi}{2}\right)\left\langle -\frac{\partial^2}{\partial g^2}\ln f_k\right\rangle \\ &= N\sin^2\left(\frac{\phi}{2}\right)\int -f_k\left(\frac{\partial^2}{\partial g^2}\ln f_k\right)dq. \end{aligned} \tag{A3}$$

Therefore, for the case of AWVA,

$$\begin{aligned}&\frac{\partial^2}{\partial g^2}\ln f_A \\ &= \frac{\partial}{\partial g}\left\{-\frac{1}{\sigma^2}\left[q-q_0-\sigma^2 g\cot^2\left(\frac{\phi}{2}\right)\right]\right. \\ &\quad\left.\times\left[-\sigma^2\cot^2\left(\frac{\phi}{2}\right)\right]\right\}. \\ &= -\sigma^2\cot^4\left(\frac{\phi}{2}\right). \end{aligned} \tag{A4}$$

Then the Fisher information is

$$\begin{aligned}\mathcal{I}_A &= N\sin^2\left(\frac{\phi}{2}\right)\int f_A\left[\sigma^2\cot^4\left(\frac{\phi}{2}\right)\right]dq \\ &= N\sigma^2\cos^2\left(\frac{\phi}{2}\right)\cot^2\left(\frac{\phi}{2}\right)\int f_A dq \\ &= N\sigma^2\cos^2\left(\frac{\phi}{2}\right)\cot^2\left(\frac{\phi}{2}\right). \end{aligned} \tag{A5}$$

The Fisher information for PWVA can be similarly obtained as

$$\mathcal{I}_A = 4N\sigma^2\cos^2\left(\frac{\phi}{2}\right). \tag{A6}$$

It should be noticed that we made the following approximation to obtain the shift at the output shown in Eq. (10). Based on the condition of $\kappa \ll 1$, we take the Taylor expansion to first order as $e^{\pm\frac{\kappa}{2}} \approx 1 \pm \frac{\kappa}{2}$ and obtain

$$I_A^{(d)} \approx e^{-\kappa}\sin^2\left(\frac{\phi}{2}\right)\left[1+\frac{\kappa^2}{4}\cot^2\left(\frac{\phi}{2}\right)\right]|\psi(q)|^2. \tag{A7}$$

To obtain Eq. (10), we introduced $\kappa = \sqrt{4gq}$ and used $g\sigma\cot^2(\frac{\phi}{2}) \ll 1$,

$$I_A^{(d)} \approx \sin^2\left(\frac{\phi}{2}\right)e^{-\sqrt{4gq}+gq\cot^2(\frac{\phi}{2})}|\psi(q)|^2. \tag{A8}$$

If $\sqrt{4g\sigma} \ll g\sigma\cot^2(\frac{\phi}{2})$ can be satisfied, the term $-\sqrt{4gq}$ can be omitted. Therefore, we get $4\tan^4(\frac{\phi}{2}) \ll g\sigma \ll \tan^2(\frac{\phi}{2})$, defining the dynamic range for our proposed protocol. The smaller $\phi$ is, the larger the number of orders it covers is.


[1] Y. Aharonov, D. Z. Albert, and L. Vaidman, Phys. Rev. Lett. **60**, 1351 (1988).
[2] A. N. Jordan, J. Martínez-Rincón, and J. C. Howell, Phys. Rev. X **4**, 011031 (2014).
[3] G. I. Viza, J. Martínez-Rincón, G. B. Alves, A. N. Jordan, and J. C. Howell, Phys. Rev. A **92**, 032127 (2015).
[4] S. Pang, J. Dressel, and T. A. Brun, Phys. Rev. Lett. **113**, 030401 (2014).
[5] D. J. Starling, P. B. Dixon, A. N. Jordan, and J. C. Howell, Phys. Rev. A **82**, 063822 (2010).
[6] O. Hosten and P. Kwiat, Science **319**, 787 (2008).
[7] M. Pfeifer and P. Fischer, Opt. Express **19**, 16508 (2011).
[8] X. Zhou, Z. Xiao, H. Luo, and S. Wen, Phys. Rev. A **85**, 043809 (2012).
[9] P. B. Dixon, D. J. Starling, A. N. Jordan, and J. C. Howell, Phys. Rev. Lett. **102**, 173601 (2009).
[10] J. M. Hogan, J. Hammer, S.-W. Chiow, S. Dickerson, D. M. S. Johnson, T. Kovachy, A. Sugarbaker, and M. A. Kasevich, Opt. Lett. **36**, 1698 (2011).
[11] M. D. Turner, C. A. Hagedorn, S. Schlamminger, and J. H. Gundlach, Opt. Lett. **36**, 1479 (2011).
[12] W. T. Liu, J. Martínez-Rincón, G. I. Viza, and J. C. Howell, Opt. Lett. **42**, 903 (2017).
[13] A. Feizpour, X. Xing, and A. M. Steinberg, Phys. Rev. Lett. **107**, 133603 (2011).
[14] X. Y. Xu, Y. Kedem, K. Sun, L. Vaidman, C. F. Li, and G. C. Guo, Phys. Rev. Lett. **111**, 033604 (2013).
[15] G. Jayaswal, G. Mistura, and M. Merano, Opt. Lett. **39**, 6257 (2014).
[16] G. I. Viza, J. Martínez-Rincón, G. A. Howland, H. Frostig, I. Shomroni, B. Dayan, and J. C. Howell, Opt. Lett. **38**, 2949 (2013).
[17] N. Brunner and C. Simon, Phys. Rev. Lett. **105**, 010405 (2010).
[18] G. Strübi and C. Bruder, Phys. Rev. Lett. **110**, 083605 (2013).
[19] O. S. Magaña-Loaiza, M. Mirhosseini, B. Rodenburg, and R. W. Boyd, Phys. Rev. Lett. **112**, 200401 (2014).
[20] J. Martínez-Rincón, W. T. Liu, G. I. Viza, and J. C. Howell, Phys. Rev. Lett. **116**, 100803 (2016).
[21] P. Egan and J. A. Stone, Opt. Lett. **37**, 4991 (2012).
[22] A. N. Jordan, P. Lewalle, J. Tollaksen, and J. C. Howell, Quantum Stud.: Math. Found. **6**, 169 (2019).
[23] G. C. Knee and E. M. Gauger, Phys. Rev. X **4**, 011032 (2014).
[24] C. Ferrie and J. Combes, Phys. Rev. Lett. **112**, 040406 (2014).
[25] A. Nishizawa, K. Nakamura, and M.-K. Fujimoto, Phys. Rev. A **85**, 062108 (2012).
[26] O. S. Magaña-Loaiza, J. Harris, J. S. Lundeen, and R. W. Boyd, Phys. Scr. **92**, 023001 (2017).
[27] K. Lyons, J. Dressel, A. N. Jordan, J. C. Howell, and P. G. Kwiat, Phys. Rev. Lett. **114**, 170801 (2015).

[28] Y. T. Wang, J. S. Tang, G. Hu *et al.*, Phys. Rev. Lett. **117**, 230801 (2016).

[29] J. C. Howell, D. J. Starling, P. B. Dixon, P. K. Vudyasetu, and A. N. Jordan, Phys. Rev. A **81**, 033813 (2010).

[30] J. Dressel, M. Malik, F. M. Miatto, A. N. Jordan, and R. W. Boyd, Rev. Mod. Phys. **86**, 307 (2014).

[31] Here $\langle q \rangle = \frac{\int q I^{(d)}(g,q)dq}{\int I^{(d)}(g,q)dq}$ is the expectation value of $q$ over the output intensity distribution, which shows the peak position of the output intensity profile since the output takes Gaussian shape.

[32] G. I. Viza, J. Martínez-Rincón, W. T. Liu, and J. C. Howell, Phys. Rev. A **94**, 043825 (2016).